Intermetallics 84 (2017) 20–24

Contents lists available at ScienceDirect

Intermetallics

journal homepage: www.elsevier.com/locate/intermet

Serration behavior and negative strain rate sensitivity of $Al_{0.1}CoCrFeNi$ high entropy alloy

Mageshwari Komarasamy, Karthik Alagarsamy, Rajiv S. Mishra*

Advanced Materials and Manufacturing Processes Institute, Department of Materials Science and Engineering, University of North Texas, Denton, TX 76203, USA

ARTICLE INFO

Article history:
Received 25 August 2016
Received in revised form
13 October 2016
Accepted 23 December 2016
Available online 4 January 2017

Keywords:
High-entropy alloy
Mechanical properties
Work-hardening
Strain-aging
Dislocations

ABSTRACT

Temperature dependent deformation mechanism of $Al_{0.1}CoCrFeNi$ high entropy alloy (HEA) was studied using monotonic and strain rate jump tests at various test temperatures in a coarse-grained single phase FCC HEA. The tensile properties of $Al_{0.1}CoCrFeNi$ HEA exhibited a modest temperature dependence in the tested range of 300–673 K. At an initial strain rate of 10^{-5} s^{-1}, the serration type was a function of the test temperature. Furthermore, the strain rate sensitivity of the flow stress changed from positive to zero to negative once the unstable plastic deformation region due to dynamic strain aging was attained.

1. Introduction

Complex concentrated alloys, particularly high entropy alloys (HEAs), are the new class of alloys with a minimum of 5 elements in equi-molar or non-equimolar quantities [1–4]. Regardless of the presence of multitude of elements, certain HEAs crystallize in simple face-centered cubic [1–3] or body-centered cubic [3,5] or hexagonal close-packed [6] crystal structure. HEAs possess exceptional properties ranging from extensive work hardenability due to nano-twins [7], high fatigue resistance [8,9], high cryogenic fracture toughness [10], and excellent high temperature strength. Various HEAs have also known to exhibit serrated flow, which, in most cases, is the macroscopic signature of the microscopic mechanism known as dynamic strain aging (DSA). DSA arises due to the dynamic interaction between the mobile solutes and the dislocations that are temporarily arrested at obstacles. Various studies have observed serrated flow in a few HEAs at certain temperature and strain rate combinations [11–14]. The apparent consequence of the dynamic strain aging phenomena is the negative strain rate sensitivity (SRS) of the flow stress, which arises due to the instability caused by the sudden unlocking of dislocations from the solute atmosphere. In the case of $Al_{0.3}CoCrFeNi$ HEA, Yasuda et al. [14] have observed the negative SRS at 873 K and at a strain rate of 1.7×10^{-4} s^{-1}.

The major uncertainty in the case of HEAs is that there is no clear understanding of the elements that can be considered as solute obstacles to the dislocation motion. In the current study, temperature dependent tensile properties of $Al_{0.1}CoCrFeNi$ HEA system was studied. Furthermore, both serrated flow and negative SRS related studies were also carried out.

2. Experimental procedure

2.4Al-24.35Co-24.45Cr-24.40Fe-24.40Ni (in at. %) HEA in as-cast condition was obtained from Sophisticated alloys. The material was cold rolled to 75% thickness reduction and then annealed at 1273 K for 24 h to obtain coarse grains. X-ray diffraction (XRD) and orientation imaging microscopy (OIM) studies were performed to observe the initial microstructural state. XRD analysis was performed using Rigaku III Ultima X-ray diffractometer with Cu K_α radiation of wavelength 0.1542 nm. OIM studies were carried out in a FEI Nova NanoSEM 230 interfaced with TSL software for data acquisition and analysis. The sample for the microscopy analysis was polished down to ~0.05 μm surface finish using colloidal silica suspension. The tensile samples were polished down to ~1 μm surface finish using diamond polishing solution. All the tensile tests

* Corresponding author.
E-mail address: Rajiv.Mishra@unt.edu (R.S. Mishra).

http://dx.doi.org/10.1016/j.intermet.2016.12.016
0966-9795/

were performed on a custom-built mini-tensile testing machine operated in a displacement controlled mode. A tube furnace was mounted around the specimen-grip assembly. The gage dimensions of the dog-bone shaped mini-tensile specimens were, length of ~5 mm, width of ~1.23 mm, and thickness ~1.10 mm. Monotonic tensile tests were performed at a strain rate of 1×10^{-5} s^{-1} and at RT, 473 K, 573 K and 673 K, to characterize the deformation mechanism as a function of temperature. The strain rate jump tests were done at 473 K and 573 K and between strain rates of 1×10^{-3} s^{-1} and 1×10^{-5} s^{-1}.

3. Results and discussion

The initial characterization of the microstructure after cold rolling and subsequent annealing are shown in Fig. 1. The XRD results, Fig. 1a, reveal the presence of an FCC phase. The absence of other peaks is a clear indication of the presence of single phase HEA. The lattice parameter, based on the XRD results, was calculated to be 3.58 Å. Furthermore, the grain size characterization of the annealed material is shown in Fig. 1b. The cold rolled material was annealed at higher temperature (1273 K) for longer time duration (24 h) to obtain coarse grained microstructure in order to exclude the effect of grain size on the mechanical properties. The presence of annealing twins indeed reduces the effective grain boundary spacing and will act as obstacles to the dislocation motion. Based on the OIM results, the obstacle spacing after annealing treatment varies from 20 to 165 μm. Given the large obstacle spacing and the lower fraction of closely spaced obstacles, grain size/twin spacing based strengthening contribution to the yield/flow stress will not be significant.

3.1. Temperature dependent tensile properties

Fig. 2 shows the temperature dependence of tensile properties at a strain rate of 10^{-5} s^{-1}. The results are summarized in Table 1. The tensile properties of $Al_{0.1}$CoCrFeNi HEA exhibited a modest temperature dependence. The yield strength can be decomposed into the following strength contributions:

$$\sigma_Y = (\sigma_{FS} + \sigma_{SS}) + \sigma_{G.B} + \sigma_{DIS} + \sigma_{PPT} \quad (1)$$

where σ_{FS} is the lattice friction stress, σ_{SS} is the solid solution strengthening, $\sigma_{G.B}$ is the strengthening arising from grain boundaries, σ_{DIS} is the dislocation strengthening, and σ_{PPT} is the strengthening due to precipitates. The strength contributions that are in the parenthesis contribute to the thermal part and the remaining ones mostly contribute to the athermal part. The general equation describing the above mentioned concept is, $\sigma_{YS} = \sigma_{thermal} + \sigma_{athermal}$. In the current study, a model microstructure was chosen with coarse grains and low dislocation density to lower the athermal contribution to the yield strength. In the case of the temperature dependent part, the dislocation glide is thermally activated, meaning that these obstacles can be overcome with the aid of temperature. Furthermore, a large lattice friction stress values were reported for HEAs, which signifies a significant variation in the lattice structure and dislocation mobility in HEAs as compared with conventional FCC alloys [15]. Wu et al. [13] have observed a severe temperature dependence of tensile properties in CoCrFeMnNi HEA and concluded that the large P-N barrier is the reason for the observed temperature dependence. In a previous study [16], we have observed a low activation volume of dislocations and explained it based on a varying Peierls barrier height rather than large energy barriers. Therefore, in the current study, the temperature dependency of the yield stress indeed stems from the fluctuation in Peierls barrier height as a function of temperature. With increased temperature contribution, the dislocations are able to overcome the thermal obstacles. Hence, the yield strength (YS) reduces with the temperature. Moreover, the work hardening is also temperature dependent as the work hardening rate is the difference between the dislocation creation rate, θ_h, and annihilation rate (dynamic recovery) θ_r, and is given as follows: $\theta = \theta_h - \theta_r(\varepsilon, \dot{\varepsilon}, T)$. The dynamic recovery is a strong function of strain rate, temperature, and SFE of the material. The work hardening behavior at various temperature was obtained by fitting the following equation in the true stress-strain curves:

$$\sigma = \sigma_y + k\varepsilon^n \quad (2)$$

where σ_y is the yield strength, k is the strength coefficient (which is material's strength at $\varepsilon = 1$), and n is the strain hardening exponent. The n and k results obtained from the above calculations are listed in Table 1. A larger n value of 0.9 at room temperature has been observed. Even with the increase in test temperature, the n value remained relatively large. Strain hardening exponent of 0.82 and a uniform elongation of 49% were observed at 673 K which is unique as compared with the conventional FCC metals and alloys. A large n value is an indication of increased capacity for dislocation storage, hence large work hardenability of the material. In the case of CG Cu, which is known to have large work hardenability, n value of 0.35

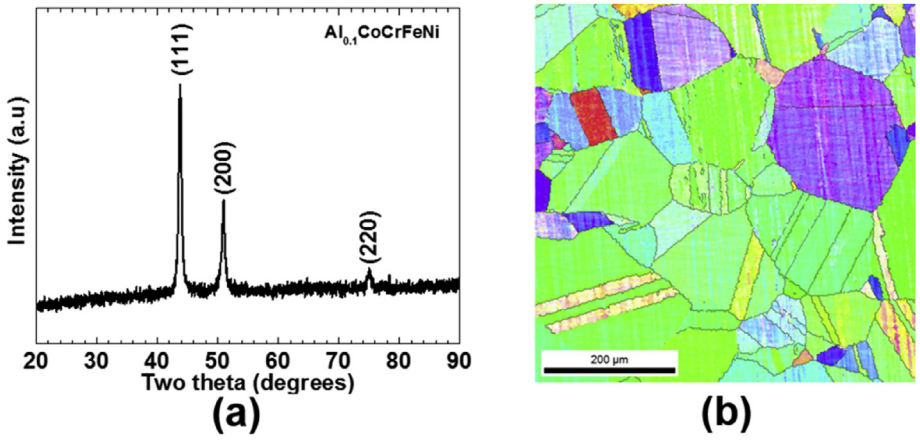

Fig. 1. (a) XRD peaks show the presence of single phase FCC and (b) OIM micrograph exhibiting a coarse-grain structure with twins.

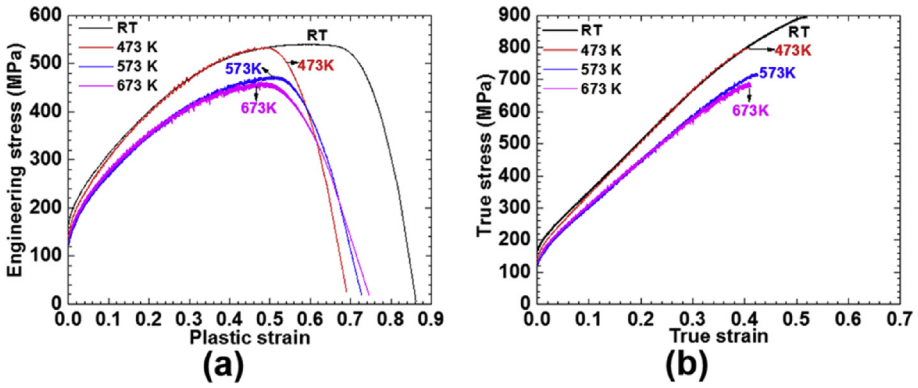

Fig. 2. (a) Engineering stress-engineering strain, and (b) true stress-true strain curves as a function of testing temperature. Note the exceptional work hardening and large uniform elongation.

was reported [17]. On the other hand, in the case of ultrafine grained Cu with nano-twins, n value of 0.66 at the twin thickness of 4 nm was observed [18]. The reason for high n value in the presence of nano-twins is due to dislocation-nano-twin interaction and the resultant large intragranular dislocation storage at twin boundary interfaces. In the current study, even a much larger n value has been observed, which increased the ductility of the material by delaying the onset of neck formation. Twinning deformation was also observed in a few HEAs at various deformation conditions [7], which is the main reason for the observed large work hardenability. The low activation volume of dislocations in HEAs is due to the high density of intrinsic obstacles which can also lead to increased dislocation storage because of higher dislocation-dislocation intersection. This in turn results in large work hardenability. The uniform elongation which depends on the work hardening capacity of the alloy stayed high at all temperatures used in this study. As discussed before, the extensive work hardening in FCC HEAs is mainly due to deformation twinning and the subsequent interaction of dislocations with the deformation twins. Zaddach et al. [19] observed that stacking fault energy (SFE) decreased with the increase in the number of elements in the equi-atomic entropy alloys and the SFE values for the quinary HEAs are in the twinning induced plasticity regime. Furthermore, Huang et al. [20] investigated the temperature dependent SFE of CoCrFeMnNi HEA and observed that the SFE increased with temperature. Consequently, the twinning probability reduces with the increase in temperature. With the reduction in the fraction of deformation twins, the dislocation-twin interaction is also reduced which will reduce the work hardening. Another point to note is the observation of serrations in the stress-strain curve in the samples tested above the room temperature. The serrations are due to the localized plastic instability and promotes premature necking instability [21]. All these factors will adversely affect the uniform elongation. Few other studies performed on various high entropy alloys have also displayed a decrease in uniform elongation as a function of temperature [13,22].

3.2. Dynamic strain aging

DSA phenomena arising from Portevin-Le Chatelier effect has, so far, successfully explained the serration behavior in many alloy systems, including high entropy alloys. The critical strain for the onset of serrations depends immensely on the strain rate, temperature, and vacancy migration energy. For a given strain rate, the critical strain will decrease with the increase in test temperature. DSA is due to the competition between the solute mobility and the dislocation velocity. In the case of high entropy alloys, the presence of serrated flow has been reported in a few studies [11–14]. When tested at 873 K and at 1.7×10^{-4} s^{-1}, $Al_{0.3}$CoCrFeNi exhibited serrated plastic flow and CoCrFeNi exhibited uniform stress-stain behavior [14]. Similarly, $Al_{0.5}$CoCrCuFeNi exhibited serrated flow at various temperature and strain rate combinations [11]. As shown in Fig. 3, serrations were observed in the present study in various conditions: at 10^{-5} s^{-1} strain rate and at temperatures of 473 K, 573 K and 673 K. Multiple serration types were observed at various strain and temperature range. The conclusion on the serration type in this study was made based on the appearance of the load/stress drop in the stress-strain curve [23–25]. At low temperatures and/or high strain rates, the solute mobility is limited and/or the dislocation velocity is high, both of which reduce the frequency and the extent of dynamic aging of dislocations by the mobile solutes. Hence, the locking/unlocking events and the frequency of the serrations on the stress-strain curve are relatively low. This is called as Type A serrations. On the other hand, in the case of higher temperature, the solute mobility is enhanced, which promotes the instantaneous locking of dislocations temporarily arrested at the obstacles by the diffusing solutes. Hence, a high frequency of serrations can be observed. This is referred as Type B or C serrations. This explanation holds good even in the case of serrated flow in HEAs, as a low and high frequency of serrations were observed at 473 K and 573 or 673 K, respectively, and at 10^{-5} s^{-1} strain rate. Type A serrations were observed at 473 K and Type B or C mixed with A + B type serrations were observed at slightly increased temperatures of 573 and 673 K.

Table 1
Summary of the temperature dependence of the tensile properties.

Temperature (K)	YS (MPa)	UTS (MPa)	UTS-YS (MPa)	UE (%)	n	k (MPa)
RT	167	895	728	60	0.90	1466
473	140	798	658	49	0.88	1468
573	124	717	593	52	0.85	1253
673	129	686	557	49	0.82	1180

UTS: Ultimate tensile strength and UE: Uniform elongation.

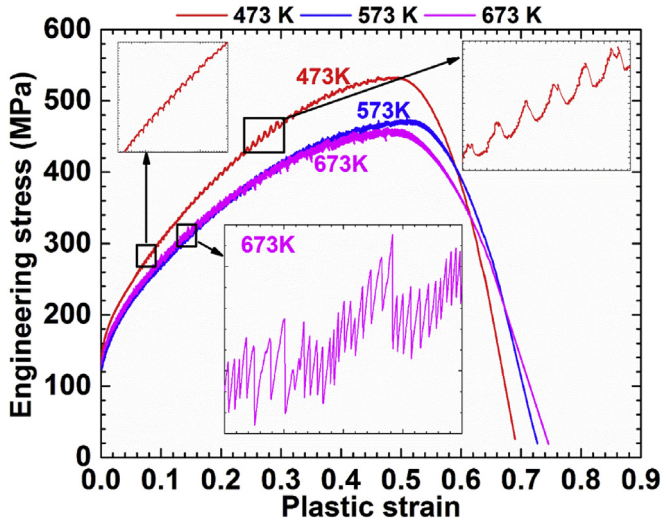

Fig. 3. Engineering stress – engineering strain curves displaying serrated flow at a strain rate of 10^{-5} s^{-1}.

3.3. Temperature dependent strain rate sensitivity

The major manifestations of the serrated flow is the negative SRS, positive temperature dependence of flow stress, and reduction in ductility. Fig. 4 shows the strain rate jump tests and the variation in rate sensitivity as a function of temperature and strain. In the current study only the up jumps, that is the strain rate change from 10^{-5} s^{-1} to 10^{-3} s^{-1} are considered. The increase in flow stress upon the rate jump from the strain rates of 10^{-5} s^{-1} to 10^{-3} s^{-1} is considered as positive SRS. And if the flow stress does not change after the rate jump, then it is called as zero SRS. Finally, the flow stress decrease upon the strain rate jump from 10^{-5} s^{-1} to 10^{-3} s^{-1} is called as negative SRS. At 473 K and in the small strain regime, a positive SRS was observed as shown in Fig. 4b. And at 573 K, zero and negative SRS were observed at small and large strain regimes, respectively, and are shown in Fig. 4(c) and (d). Both the strain rate regions are marked clearly on the stress-strain curves in Fig. 4 to distinguish all three strain rate sensitivities. The variation in rate sensitivity from positive to negative is due to the change in deformation mode from homogeneous to inhomogeneous serrated plastic flow initiated due to the dynamic interaction between the dislocations and the solutes. Negative SRS is always correlated with the DSA of dislocations by the solutes. In the current study, even though the serrations were observed at small strains at 573 K (Fig. 4c), the instability to create a negative SRS was not attained. Therefore, in order to observe the effect of negative SRS on the macro-scale, a critical number of locking and unlocking events of certain magnitude may be a necessary requirement. Hence, there is a critical strain which is larger than the onset strain for serrated plastic flow, is required for the occurrence of negative SRS of the flow stress. In the current study, the negative SRS was observed at 573 K. Since serrated flow was observed until 673 K, the presence of negative SRS at this temperature is anticipated. In general, inhomogeneous plastic flow is usually observed in certain strain rate and temperature regime. Therefore, if the test temperature is raised above 673 K, there is possibility for uniform plastic flow which will remove the negative SRS and bring back the positive SRS. There are studies on a few HEAs where the transition from homogeneous to inhomogeneous to homogeneous plastic deformation with the increase deformation temperature was observed [13,14]. In the case of, $Al_{0.3}CoCrFeNi$ HEA single crystals, inhomogeneous plastic deformation was observed at 873 K and 1073 K, and uniform plastic flow was observed at 1273 K and also at temperatures below 873 K [14].

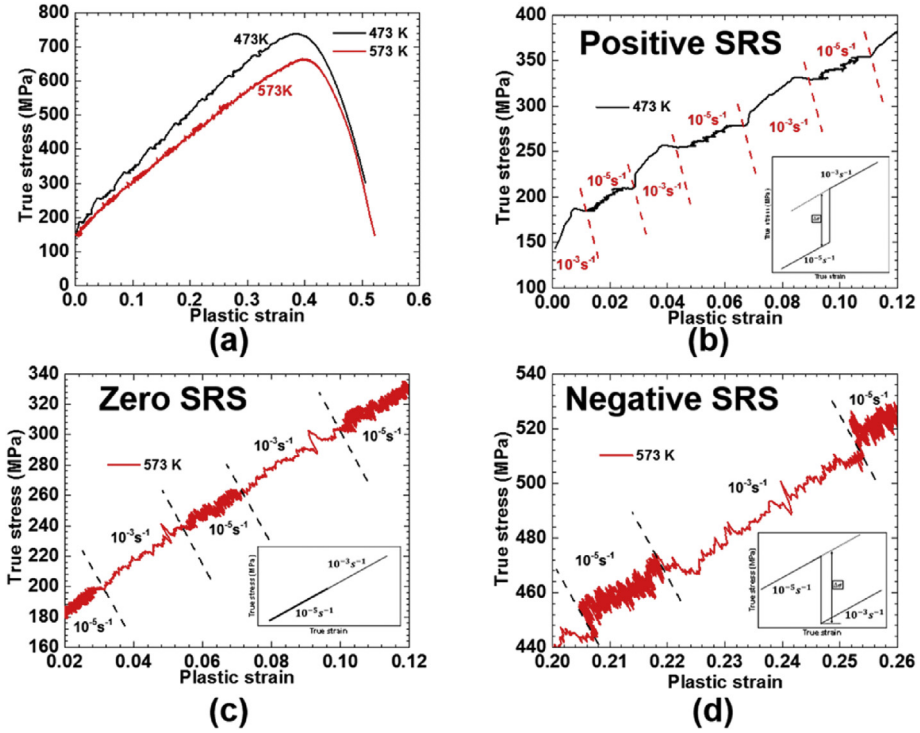

Fig. 4. (a) True stress – true strain curves showing the rate jump tests performed at 473 K and 573 K, magnified regions showing (b) positive SRS at 473 K, (c) zero SRS at 573 K and at small plastic strain, and (d) negative SRS at 573 K and at large plastic strain. The dashed lines in Figures (b), (c), and (d) denote various strain rate regions. The insets in Figures (b), (c), and (d) are the schematics of positive SRS, zero SRS, and negative SRS, respectively.

4. Conclusion

In the present work, we have studied temperature dependent deformation mechanisms of a coarse-grained $Al_{0.1}$CoCrFeNi HEA at various test conditions. The HEA exhibited temperature dependent YS, UTS and work hardening coefficient. Inhomogeneous plastic flow started at the temperature of 473 K and at an initial strain rate of 10^{-5} s^{-1}. Depending on the testing temperature, various types of serrations were observed in the stress-strain curve. The macroscopic indication of the microscopic DSA phenomena is the negative strain sensitivity of the flow stress, which was observed at 573 K. The critical plastic strain to initiate negative SRS is larger than the onset strain for serrations.

Acknowledgments

We would like to thank Center for Advanced Research and Technology (CART) for the microscopy facilities.

References

[1] J.W. Yeh, S.K. Chen, S.J. Lin, J.Y. Gan, T.S. Chin, T.T. Shun, Nanostructured high-entropy alloys with multiple principal elements: novel alloy design concepts and outcomes, Adv. Eng. Mater. 6 (2004) 299–303.
[2] B. Cantor, I.T.H. Chang, P. Knight, A.J.B. Vincent, Microstructural development in equiatomic multicomponent alloys, Mater. Sci. Eng. A 375–377 (2004) 213–218.
[3] Y. Zhang, T.T. Zuo, M.C. Gao, K.A. Dahmen, P.K. Liaw, Z.P. Lu, Microstructures and properties of high-entropy alloys, Prog. Mater. Sci. 61 (2014) 1–93.
[4] J.Y. He, W.H. Liu, H. Wang, Y. Wu, X.Y. Liu, T.G. Nieh, Z.P. Lu, Effects of Al addition on structural evolution and tensile properties of the FeCoNiCrMn high-entropy alloy system, Acta Mater. 62 (2014) 105–113.
[5] Y.J. Zhou, Y. Zhang, Y.L. Wang, G.L. Chen, Solid solution alloys of $AlCoCrFeNiTi_x$ with excellent room-temperature mechanical properties, Appl. Phys. Lett. 90 (2007).
[6] Y.J. Zhao, J.W. Qiao, S.G. Ma, M.C. Gao, H.J. Yang, M.W. Chen, Y. Zhang, A hexagonal close-packed high-entropy alloy: the effect of entropy, Mater. Des. 96 (2016) 10–15.
[7] M. Komarasamy, N. Kumar, Z. Tang, R.S. Mishra, P.K. Liaw, Effect of microstructure on the deformation mechanism of friction stir-processed $Al_{0.1}$CoCrFeNi high entropy alloy, Mater. Res. Lett. 3 (2015) 30–34.
[8] M.A. Hemphill, T. Yuan, G.Y. Wang, J.W. Yeh, C.W. Tsai, A. Chuang, P.K. Liaw, Fatigue behavior of $Al_{0.5}$CoCrCuFeNi high entropy alloys, Acta Mater. 60 (2012) 5723–5734.
[9] Z. Tang, T. Yuan, C.W. Tsai, J.W. Yeh, C.D. Lundin, P.K. Liaw, Fatigue behavior of a wrought $Al_{0.5}$CoCrCuFeNi two-phase high-entropy alloy, Acta Mater. 99 (2015) 247–258.
[10] B. Gludovatz, A. Hohenwarter, D. Catoor, E.H. Chang, E.P. George, R.O. Ritchie, A fracture-resistant high-entropy alloy for cryogenic applications, Science 345 (2014) 1153–1158.
[11] S. Chen, X. Xie, B. Chen, J. Qiao, Y. Zhang, Y. Ren, K.A. Dahmen, P.K. Liaw, Effects of temperature on serrated flows of $Al_{0.5}$CoCrCuFeNi high-entropy alloy, JOM 67 (2015) 2314–2320.
[12] J. Antonaglia, X. Xie, Z. Tang, C.W. Tsai, J.W. Qiao, Y. Zhang, M.O. Laktionova, E.D. Tabachnikova, J.W. Yeh, O.N. Senkov, M.C. Gao, J.T. Uhl, P.K. Liaw, K.A. Dahmen, Temperature effects on deformation and serration behavior of high-entropy alloys (HEAs), JOM 66 (2014) 2002–2008.
[13] Z. Wu, H. Bei, G.M. Pharr, E.P. George, Temperature dependence of the mechanical properties of equiatomic solid solution alloys with face-centered cubic crystal structures, Acta Mater. 81 (2014) 428–441.
[14] H.Y. Yasuda, K. Shigeno, T. Nagase, Dynamic strain aging of $Al_{0.3}$CoCrFeNi high entropy alloy single crystals, Scr. Mater 108 (2015) 80–83.
[15] N. Kumar, M. Komarasamy, P. Nelaturu, Z. Tang, P.K. Liaw, R.S. Mishra, Friction stir processing of a high entropy alloy $Al_{0.1}$CoCrFeNi, JOM 67 (2015) 1007–1013.
[16] M. Komarasamy, N. Kumar, R.S. Mishra, P.K. Liaw, Anomalies in the deformation mechanism and kinetics of coarse-grained high entropy alloy, Mater. Sci. Eng. A 654 (2016) 256–263.
[17] A. Misra, X. Zhang, D. Hammon, R.G. Hoagland, Work hardening in rolled nanolayered metallic composites, Acta Mater. 53 (2005) 221–226.
[18] L. Lu, Z.S. You, K. Lu, Work hardening of polycrystalline Cu with nanoscale twins, Scr. Mater. 66 (2012) 837–842.
[19] A.J. Zaddach, C. Niu, C.C. Koch, D.L. Irving, Mechanical properties and stacking fault energies of NiFeCrCoMn high-entropy alloy, JOM 65 (2012) 1780–1789.
[20] S. Huang, W. Li, S. Lu, F. Tian, J. Shen, E. Holmström, L. Vitos, Temperature dependent stacking fault energy of FeCrCoNiMn high entropy alloy, Scr. Mater. 108 (2015) 44–47.
[21] J. Kang, D.S. Wilkinson, J.D. Embury, M. Jain, A.J. Beaudoin, Effect of type-B Portevin–Le Chatelier bands on the onset of necking in uniaxial tension of strip cast AA5754 sheets, Scr. Mater. 53 (2005) 499–503.
[22] A. Gali, E.P. George, Tensile properties of high- and medium-entropy alloys, Intermetallics 39 (2013) 74–78.
[23] A. Yilmaz, The Portevin–Le Chatelier effect: a review of experimental findings, Sci. Technol. Adv. Mater. 12 (2011) 1–16.
[24] H. Halim, D.S. Wilkinson, M. Niewczas, The Portevin–Le Chatelier (PLC) effect and shear band formation in an AA5754 alloy, Acta Mater. 55 (2007) 4151–4160.
[25] P. Rodriguez, Serrated plastic flow, Bull. Mater. Sci. 6 (1984) 653–663.